Measurement 183 (2021) 109867

Contents lists available at ScienceDirect

Measurement

journal homepage: www.elsevier.com/locate/measurement

Low-frequency noise measurements of IR photodetectors with voltage cross correlation system

Krzysztof Achtenberg [a,*], Janusz Mikołajczyk [a], Carmine Ciofi [b], Graziella Scandurra [b], Krystian Michalczewski [c], Zbigniew Bielecki [a]

[a] Institute of Optoelectronics, Military University of Technology, Kaliskiego Str. 2, 00908 Warsaw, Poland
[b] Department of Engineering, University of Messina, c.da di Dio, 98166 Messina, Italy
[c] VIGO System S.A., Poznanska Str. 129/133, 05-850 Ożarów Mazowiecki, Poland

ARTICLE INFO

Keywords:
Noise measurements
Low frequency noise
Cross-correlation
Low noise amplifier
IR photodetector
QLSA

ABSTRACT

The paper presents a system for noise measurements in infrared photodetectors characterized by low shunt resistances based on a two-channel ultra-low-noise voltage amplifier with paralleled discrete JFETs at the input stages. Using cross correlation method, a background noise well below of 10^{-19} V^2/Hz can be obtained at frequencies above 10 Hz. To facilitate the estimation of the noise in such a wide frequency range (5 decades), we also developed a software based on the QLSA library. As a result of these efforts, the equivalent input voltage noise of the system is below 10^{-19} V^2/Hz at 10 Hz and 10^{-20} V^2/Hz for frequencies above a few hundred Hz. The system effectiveness is demonstrated by noise measurements at room temperature on advanced $InAs_xSb_{1-x}$ photodetectors characterized by an active area of 1 mm^2 and a shunt resistance below 10 Ω.

1. Introduction

Noise measurements, and especially Low Frequency Noise Measurements (LFNM) provide for a very sensitive technique for the investigation of the quality and reliability of electron devices and materials [1]. Since voltage and current fluctuations across a biased device depend on the microscopic interaction of the charge carrier with the active regions of the devices, the analysis of the noise in proper condition can be quite helpful in understanding in the development of accurate conduction models [2]. Moreover, defects in the microstructure of the devices influence the level and the shape of the noise spectrum that can then be used for obtaining information on the quality of the device production process. Often microscopic defects result in the formation of localized energy levels within the forbidden gap of a semiconductor, and the trapping-detrapping of charge carriers may result in current fluctuations usually referred to as generation-recombination (g-r) noise [3]. In addition, the investigation of the shot noise can provide information on whether transport through a potential barrier occurs because of clean tunnelling or trap-assisted tunnelling. All this information can be especially valuable in the development Infrared (IR) detectors, as LFNM are very sensitive the manufacturing steps and monitoring the low frequency noise can help in improving the production process and, hence, the overall quality of the devices. It is for this reason that noise in IR detectors has been under investigation for years. To obtain optimum performance IR detectors often require working in carefully selected bias conditions. The limit to the detectivity for the detector is usually set by the flicker noise superimposed to the signal. This noise is determined by the detector operation conditions and is highly dependent on bias voltage and temperature. While in actual applications, the bias system may introduce noise that limits the detectivity, the ultimate limit is set by the noise generated by the IR detector itself, and for this reason, that is extremely important to be able to separate the noise generated by the device from other noise contributions in the circuit. More in general, noise measurements in IR detectors can be used for assessing the performances of such devices in terms of detectivity, quality, and reliability [1,4].

Typically, the overall current noise spectrum through a device biased at constant voltage depends on the temperature and the bias level and is the result of the contribution of thermal noise, shot noise, flicker (or $1/f$) noise, and g-r noise. As fare the investigation of the quality and reliability of the devices are concerned, the most interesting noise component are the flicker noise and the g-r noise. Pure g-r noise manifests itself in the form of a Lorentzian spectrum, however, it is often observed in conjunction with flicker noise. The presence of g-r components

* Corresponding author.
E-mail address: krzysztof.achtenberg@wat.edu.pl (K. Achtenberg).

https://doi.org/10.1016/j.measurement.2021.109867
Received 22 February 2021; Received in revised form 29 June 2021; Accepted 6 July 2021
Available online 10 July 2021

superimposed to flicker noise can be recognized because of the presence of characteristic "bumps" in the shape of the low frequency noise [5]. The separation of the Lorentzian components from the pure flicker noise in actual noise measurements can be performed by resorting to proper mathematical models and numerical extraction procedures [6,7].

Performing accurate LFNM is never an easy task, but in the case of IR detectors characterized by shunt resistances in the order of a few Ohms at room temperature, it becomes particularly challenging [8]. In this type of detector, that because of the low shunt resistances are biased with low DC voltages, the level of the generated noise is extremely low and, at least in the case of commercially available instrumentation, can be well below the flicker noise introduced by the measurement system itself. In order to achieve the goal of reliable estimating the flicker noise component in IR photodetectors with very low biases (a few mV) almost always required the careful design of dedicated instrumentation characterized by very low levels of background noise. In some cases, the use of cross correlation approaches in noise measurement can result beneficial, especially at very low bias levels [9].

In this paper, we discuss the design of ultra-low noise measurement systems specifically targeted at the investigation of the noise generated in IR detectors characterized by very low shunt resistance. In particular, we will demonstrate that excellent performances can be obtained in a reasonable measurement time if the cross correlation approach is employed in conjunction with very low noise preamplifiers. In the first section, we will address the problem of the selection of the most appropriate measurement configuration. Next, we discuss the design of ultra-low-noise amplifiers for the implementation of the cross correlation approach in a voltage noise measurement configuration. Finally, in the experimental section, we discuss the result of the tests that confirm the effectiveness of the approach we propose. The results that can be obtained are compared with others reported in the literature, and the result of measurement on actual low-shunt resistance IR photodetectors will be presented.

2. Material and methods

To analyze the main issues that need to be faced in the measurement of the Power Spectral Density (PSD) of the noise across the devices we are interested in, we start from the observation that, with shunt resistances as low as a few ohms, the PSD of the noise generated by the device, at thermal equilibrium, is typically below the Background Noise (BN) of most low noise measurement systems. The situation is schematically illustrated in Fig. 1a for the case of voltage noise measurements. The measured noise (red curve) is the result of the combination of the detector noise and the measurement system BN. The detector noise, when no bias is applied, coincides with the thermal voltage noise of its equivalent resistance. On the other hand, the BN introduced by the measurement system (that is based on biased active electronic devices) displays a flicker component ($1/f$) that is dominant at lower frequencies. For increasing frequencies, we are left with a dominant white noise component until the bandwidth limit of the measurement system is reached, and we observe a fictitious reduction of the noise. If the detector is biased, the most important change that we should observe is the appearance of a flicker component in the noise generated by the Device Under Test (DUT), as shown in Fig. 1b. However, unless the flicker noise generated by the DUT becomes much larger than the noise introduced by the measurement system, it is not easy to obtain its correct estimation. It must be noted that the flicker noise is often the most important noise component for the evaluation of the quality and reliability of electron devices [10]. If the bias increases, the flicker noise component generated by the DUT increases as well, and we can reach a situation in which the noise introduced by the measurement system becomes negligible, at least in the lowest frequency range (Fig. 1c). By further increasing the bias, a situation can be reached in which the noise generated by the measurement system may become negligible at all frequencies, as in Fig. (1d). Clearly, for the same DUT, the bias level for which reliable PSD estimation can be obtained at a given frequency depends on the BN at that frequency. It is therefore mandatory to obtain a BN as low as possible to maintain the ability to explore the noise behaviour at different bias level and in order not to damage the DUT by applying excessive bias. Extremely interesting features such as the presence of Lorentzian components [11] superimposed to the flicker noise and their dependence on temperature and bias can only be analysed if reliable noise measurements are possible in an extended bias range.

Depending on the specific characteristics of the DUT, the most appropriate noise measurement system and devices must be selected, with a careful selection of all its components [12]. The block scheme of the most common noise measurement configurations is reported in Fig. 2. The DUT can be biased by a constant voltage source for current noise measurements or by a constant current source for voltage noise measurements. The noise introduced by these current or voltage sources employed to bias the DUT contributes to the BN of the measurement systems and therefore, great care must be taken into its minimization. Often, batteries are employed for the implementation of the voltage sources V_S in Fig. 2. In the case of the configuration for voltage noise measurement (Fig. 2a), if the resistance R_B is much larger than the equivalent impedance of the DUT, the series combination of V_S and R_B behaves as a current source, in the case of the current noise measurement (Fig. 2b), the virtual short at the input of the Trans-Impedance Amplifier (TIA) allows to set the bias voltage across the DUT to V_S. In some cases, to increase flexibility in changing the bias value, filtered lab power supplies or special designed low-noise circuits [13,14] can be employed. In the case of voltage noise measurements, the voltage noise fluctuations across the DUT are amplified using a low-noise Voltage Amplifier (VA), while in the case of current noise measurements, a low-noise TIA must be used. The amplified voltage signal, both in the case of a VA (with gain of A_V) or of a TIA (with gain of A_R), is sent either to a benchtop spectrum analyzer or to a computer based acquisition system (DAQ) with an anti-aliasing filter (AAF) and analog to digital converter (ADC) for power spectral evaluation.

In all cases, the amplification must be large to rise the noise signal generated by the DUT to a level compatible with the input range of the spectrum estimation system. This poses the problem or removing the DC component of the signal in order not to saturate the amplifiers. In the case of a VA this is usually obtained by an AC passive coupling network between the DUT and the input of the amplifier; in the case of the TIA configuration, the transimpedance gain can be divided into a fist stage TIA with reduced gain (at the cost of higher noise), followed by an AC coupled second stage VA. Alternatively, in the case of TIA, DC compensation circuits can be used [15,16]. While there may be a preference, from the point of view of the interpretation of the data, between voltage noise and current noise measurements, if the voltage-current DC

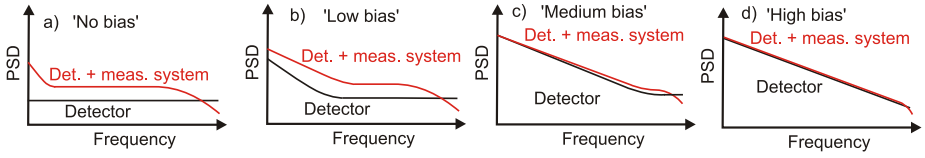

Fig. 1. Expected measured noise when the background noise of the measurement system is taken into consideration: a) refers to the case of an unbiased IR detector used as a DUT; b) to d) are relative to the increasing level of bias for the DUT.

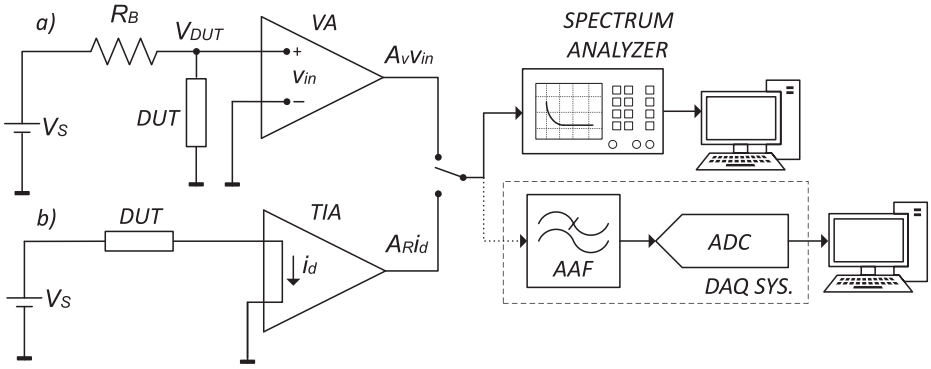

Fig. 2. Typical configuration for noise measurements of a DUT.

characteristic and the equivalent impedance of the DUT are known, current noise measurement and voltage noise measurements are, in principle, equivalent and one can be obtained from the other. However, when dealing with actual DUTs and the limitations of available devices and systems, the selection of the most proper preamp configuration (TIA or VA) is a key point in the development of a noise measurement setup. Among the parameters that may influence such a choice, the type of input stage of the amplifier (bipolar junction transistor - BJT, junction field-effect transistor - JFET or metal-oxide semiconductor field-effect transistor - MOSFET based), with the different values of equivalent input voltage noise (e_n) and current noise (i_n) plays a major role. In general terms, there is no single "optimal configuration". Rather, it is the type of DUT and its characteristics, among which the equivalent impedance plays a major role, that guides the design of the amplifier. Typically, for low impedance DUTs, it is the equivalent voltage noise e_n of the amplifier that limits the sensitivity, while the equivalent input current i_n is mainly responsible for limiting the sensitivity in the case of high impedance DUTs [17–19].

In the specific case of noise measurements on IR detectors, most of the published results are obtained employing commercially available instrumentation. In [20], the authors present a LFNM system obtained using an EG&G (model 5182 [21]) TIA, lab power supply with filter sections, and a data acquisition system. The result of noise measurements on low resistance photodetectors using the system in [20] are mentioned in [22]. A similar approach is used in [7,23,24]. Noise measurements obtained using a commercially available VA EG&G (model 5113 [25]) and a USB-based dynamic signal analyzer (Photon+) are described in articles [26,27].

In some cases, multi-channel cross correlation approaches can be used to reduce the equivalent BN of the system compared to the case in which one single amplifier is employed. In this approach, the inputs of two or more identical signal channels are connected to the same DUT and, using cross correlation between the outputs, uncorrelated noise components introduced by the amplifiers can be rejected by employing a sufficiently long averaging time [28,29]. The block diagram of a two-channel cross correlation spectrum analyzer for voltage noise measurements is shown in Fig. 3. It consists of a module with two identical amplifiers (A_1 and A_2), AAF, simultaneously sampling ADC's, and a signal processing that implements the cross correlation procedure (cross spectrum estimation) basing on discrete Fourier transform (DFT).

An example of such an approach is reported in [8], where commercially available EG&G (5186 model) VA's were used. Thanks to the cross correlation approach, lower background noise was obtained with respect to the other approaches mentioned above, and this resulted in the ability to perform meaningful voltage noise measurements on IR photodetectors characterized by lower shunt resistances. The performances of the measurement systems mentioned above are summarized in Table 1.

Some results of IR detectors' noise characteristics can be also found in other works [30–35] but no detailed information about the measurement systems was reported. In this paper we demonstrate that by means of a dedicated design a considerable improvement in the performances of a noise measurement system for low shunt impedance detectors can be obtained. After addressing the issue of the selection of the most advantageous front-end configuration for noise measurement in low impedance devices, we discuss in some detail the measurement system that we have designed, providing experimental data on actual devices as proof of its effectiveness.

3. Front end amplifier

As we have noted above, a first choice that needs to be made in designing a low noise measurement system is the selection of the front-end amplifier configuration. To this end, we will revise in some detail and general terms the noise performances of TIA and VA front-end in relation with the DUT impedance.

3.1. Trans-Impedance amplifier front-end

The most common configuration for low-noise measurements using a TIA is reported in Fig. 4. The operational amplifier OA_1 can be a monolithic device, or it can include low noise, discrete device based input stage. The overall gain of the system is the product of the transimpedance gain of the first stage multiplied by the voltage gain A_v of the

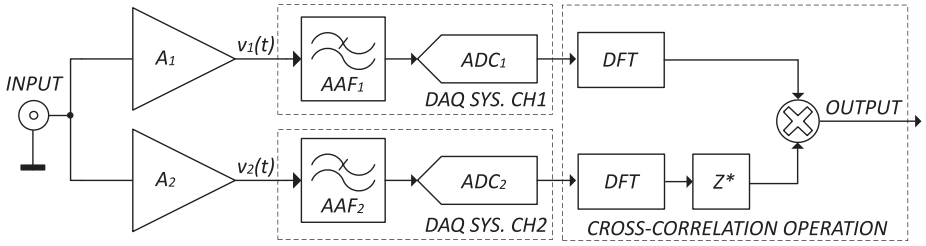

Fig. 3. Block diagram of a cross correlation spectrum analyzer (Z* - complex conjugate operation).

Table 1
Performances of the IR photodetectors noise measurements systems.

Type of the meas. Detectors*	Det. resistances	Type of measured fluctuations/method	Model of the front-end	Meas. system noise (amplifiers)	Meas. bandw.	Range of bias (rev.)	Source
InAs/InAsSb SL	≈ 5 Ω and 11 Ω [300 K]	voltage/two channels with cross correlation	SR 5186	$e_n = 1.6 \times 10^{-17}$ V^2/Hz at 1 kHz	1 Hz to 1 kHz	≈ 90 to 800 mV	[8]
HgCdTe, InAs/GaSb T2SL	≈ 60 Ω to above 1 MΩ (dynamic resistance)	current/single channel	TIA EG&G 5182	$e_n = 1 \times 10^{-17}$ A^2/Hz at 100 Hz, $i_n = 2 \times 10^{-27}$ A^2/Hz [10^8 V/A] at 1 kHz, $i_n = 2 \times 10^{-24}$ A^2/Hz [10^6 V/A] at 1 kHz	1 Hz to 10 kHz	1.5 mV to 1 V	[20]
p-InAsSbP/n-InAs	about 1 kΩ [300 K]	voltage/single channel	EG&G 5113	$e_n = 1.6 \times 10^{-17}$ V^2/Hz at 1 kHz	0.5 Hz to 10 kHz	6.4 nA to 4 mA (forw.)	[26]
p-InAsSbP/n-InAs	$R_0 \approx 10^3$ Ω [300 K]	voltage/single channel	EG&G 5113	$e_n = 1.6 \times 10^{-17}$ V^2/Hz at 1 kHz	0.5 Hz to 10 kHz	≈ 40 pA to 1 μA	[27]
InAs/GaSb SL	$R_0A = 5.3 \times 10^5$ Ωcm^2 [80 K]	current/single channel	TIA Kiethley 428	$i_n = 90$ nA$_{rms}$ at 10^3 V/A, $i_n = 1.2$ fA$_{rms}$ at 10^{11} V/A	0.3 to about 200 Hz	100 to 800 mV	[23]
InAs/GaSb SL	R_0A higher than 1×10^6 Ωcm^2 [77 K]	current/single channel	TIA DDPCA-300	$i_n = 2 \times 10^{-21}$ A^2/Hz [10^4 V/A] at 10 Hz, $i_n = 4 \times 10^{-30}$ A^2/Hz [10^{12} V/A] at 10 Hz	1 to 20 Hz	0.2 to 0.9 V	[24]
InAs/GaSb SL	–	current/single channel	TIA DLPCA-200	$e_n = 1.6 \times 10^{-17}$ V^2/Hz at 1 kHz, $i_n = 4 \times 10^{-22}$ A^2/Hz [10^3 V/A] at 10 kHz, $i_n = 1.85 \times 10^{-29}$ A^2/Hz [10^{11} V/A] at 100 Hz	1 Hz to 8 kHz	0.05 to 0.8 V	[7]

* T2SL - Type II superlattice, SL – superlattice.

second stage voltage amplifier. As we have mentioned before, the second stage is typically AC coupled to avoid saturation due to the DC component of the current flowing through the DUT. If the input stage of OA_1 is based on JFET or MOSFET devices, the effect of the equivalent current noise sources at its inverting and non-inverting input can be usually neglected, and the BN is determined by its input equivalent noise voltage source (e_n) and by the feedback resistance noise (e_{nRf}). Because of the gain of the first stage, the noise introduced by the second stage can be neglected.

For the sake of simplicity, we will assume no bandwidth limitations and that the DUT behaves as resistance with value R_{DUT}. In the virtual short circuit approximation for the OA_1 and the band-pass of the amplifier (the second stage is AC coupled to the first stage), the *trans*-resistance gain A_R is given by:

$$A_R = \frac{V_O}{i_{DUT}} = -R_F A_V. \tag{1}$$

In order to simplify the discussion, we will assume A_V to be a real number in the band-pass (constant frequency response). Assuming all noise sources uncorrelated (because arising from different devices), the output PSD of the voltage noise at the output of the system (S_{VO}) is given by:

$$S_{VO} = S_{iDUT}|R_F A_V|^2 + 4kTR_F|A_V|^2 + S_{en}\left|1 + \frac{R_F}{R_{DUT}}\right|^2 |A_V|^2 + \frac{S_{VS}}{R_{DUT}^2}|R_F A_V|^2, \tag{2}$$

where k is the Boltzmann constant, S_{VS} and S_{en} are the PSD of the noise sources e_{nVS} and e_n and S_{iDUT} is the PSD of the current noise i_{DUT}. Generally, S_{iDUT} is the superposition of the thermal noise associated to the resistance R_{DUT} and of the flicker noise that is the result of the bias. Note that, save for the thermal noise sources, the PSD of all other noise sources, in general, depends on the frequency. We have made a choice not to explicitly indicate the dependence on the frequency in order to simplify the notation, that is, we write S_x instead of $S_x(f)$, unless explicit reference to the frequency dependence is required in the discussion. From the output noise, we obtain the equivalent input current noise S_{II} dividing by the modulus of the *trans*-resistance gain squared:

$$S_{II} = \frac{S_{VO}}{|A_R|^2} = S_{iDUT} + \frac{4kT}{R_F} + S_{en}\left|\frac{1}{R_F} + \frac{1}{R_{DUT}}\right|^2 + \frac{S_{VS}}{R_{DUT}^2}. \tag{3}$$

The additional noise introduced by the *TIA* (S_{IIBN}) and bias circuit is therefore given by:

$$S_{IIBN} = \frac{4kT}{R_F} + S_{en}\left|\frac{1}{R_F} + \frac{1}{R_{DUT}}\right|^2 + \frac{S_{VS}}{R_{DUT}^2}. \tag{4}$$

This very same quantity can also be written as:

$$S_{IIBN} = \frac{1}{R_F^2}\left(4kTR_F + S_{en}\left|1 + \frac{R_F}{R_{DUT}}\right|^2 + \frac{S_{VS}R_F^2}{R_{DUT}^2}\right) \tag{5}$$

From Eq. (4) (or 5), it is apparent that the noise introduced by the transimpedance amplifier depends on the DUT impedance (R_{DUT}). In the field of LFNM, the usual application for a TIA is the current noise measurement of a DUT characterized by a high impedance. In this situation, the noise introduced by the TIA is close to the noise due to the feedback resistance alone, and it makes sense to increase R_F obtaining lower and lower S_{IIBN} as can be clearly deduced from Eq. (4). In these cases, the noise introduced by the TIA is very close to the noise measured with the input open. It is this noise (equivalent input noise with open input, i.e. with $R_{DUT} \to \infty$) that is reported in the data sheets of commercial TIAs. If, however, the input impedance is sufficiently small compared to R_F, as it can be more clearly deduced form Eq. (5), we reach a point in which it is the equivalent input noise S_{en}, together with the ratio between R_F and R_{DUT}, that sets the background noise. This has some interesting consequences.

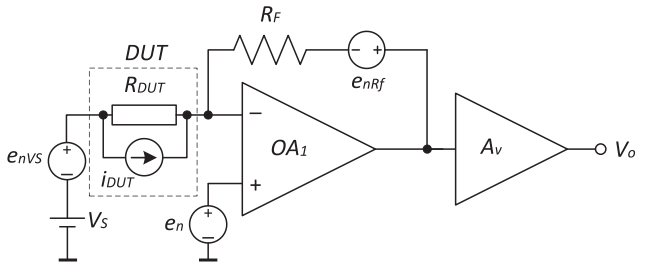

Fig. 4. Simplified equivalent circuit for noise calculation in a *trans*-resistance amplifier.

Normally, in a TIA, one increases the *trans*-resistance gain by increasing R_F to reduce the background noise (in the case of large DUT impedances). If, however, we are in a situation in which the noise due to S_{en} becomes dominant ($R_{DUT} \ll R_F$), one obtains that:

$$S_{IIBN} \approx \frac{S_{en}}{R_{DUT}^2}. \tag{6}$$

Eq. (6) essentially means that the noise introduced by the TIA does not depend on R_F. It is clear, therefore, that when we reach the situation in Eq. (6), the specifications in terms of equivalent input noise with the input open does not make much sense. If one wants to maintain the measurement configuration in Fig. 2, one must try to obtain the lowest possible value for S_{en}, with the value of the equivalent input noise with the input open being irrelevant [36]. Eq. (6) also has one notable consequence in terms of the ability to measure the thermal current noise of resistance: the PSD of the thermal current noise of resistance is proportional to the inverse of the resistance, while S_{IIBN} is proportional to the inverse of the resistance squared. This means that while the current noise of resistance increases as the resistance decreases, measuring its value with a TIA becomes increasingly difficult for lower and lower resistances because of the comparatively much larger increase in S_{IIBN}. One further observation is that it can be easily shown that if we employ the same OA_1 in Fig. 4 to set up a voltage noise measurement circuit as discussed in the next subsection, the ratio between the noise introduced by the amplifier and the "useful noise" (the one generated by the DUT) would be the same one obtained in the case of the TIA when Eq. (6) holds, thus essentially making the two approaches equivalent from the point of view of the signal to noise ratio performances.

In general, performing voltage noise measurements is easier than performing current noise measurements and this fact, combined with the fact that in terms of background noise, there is no advantage with a TIA when Eq. (6) holds, leads to the conclusion that, whenever possible, it is better to perform voltage noise measurements when dealing with low impedances. Moreover, resorting to voltage noise measurements allows an easy implementation of the cross correlation approach in Fig. 3.

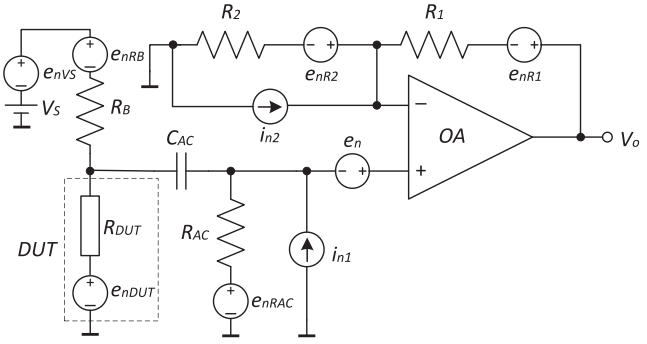

Fig. 5. Simplified equivalent circuit for noise calculation in an AC coupled voltage amplifier.

3.2. Voltage amplifier front-end

Fig. 5 shows a typical VA configuration for voltage noise measurements with a high-pass RC coupling network ($R_{AC}C_{AC}$) at the input to reject the DC voltage across the DUT due to bias. The voltage source V_S in series with R_B behaves as a current source for $R_B \gg R_{DUT}$.

In this configuration, we must take into consideration the two equivalent current noise sources (i_{n1}, i_{n2}) and the equivalent voltage noise source (e_n) due to the OA. We have also explicitly shown the voltage noise sources accounting for the thermal noise ($4kTR$) for resistors R_{AC} (e_{nRAC}), R_B (e_{nRB}), R_1 (e_{nR1}), R_2 (e_{nR2}) and for the noise introduced by the bias source V_S (e_{nVS}). In virtual short circuit approximation for the inputs of the operational amplifier, the voltage gain from the non-inverting input voltage v_+ to the output voltage V_O is given by:

$$A_V = \frac{V_O}{v_+} = 1 + \frac{R_1}{R_2}, \tag{7}$$

where v_+ means the voltage at noninverting input.

If the ratio between R_1 and R_2 remains the same, it is usually possible to reduce the value of these resistances down to a point for which their noise contribution, and the noise contribution due the i_{n2}, become negligible with respect to the other sources of noise. Because of the condition $R_B \gg R_{DUT}$, also the noise contribution from e_{nRB} can be neglected. It must be noted that in order not to attenuate the useful signal (e_{nDUT}), we must also ensure $R_{AC} \gg R_{DUT,}$ and this usually means that we cannot employ an operational amplifier with BJT input stage because of the relatively high input bias current that, flowing through R_{AC} would result in a large offset. Since we must resort to FET input stages, this means that in any case i_{n1}, i_{n2} are small, and their effect can be assumed to be negligible (note that in the passband, the impedance seen by the source i_{n2} is essentially $R_{DUT,}$ that, in the context of this work, we expect to be small). The issue of the effect of the noise introduced by the resistance R_B is more complex, but it can be demonstrated that if the frequency corner set by R_{AC} and C_{AC} is set to be well below the minimum frequency of interest, also the noise contribution by R_{AC} can be neglected [16]. With these assumptions, that are almost always verified, and assuming, for the sake of simplicity, no upper bandwidth limitations, for the PSD of the output voltage noise we have:

$$S_{VO} = S_{enDUT}|A_V|^2 + S_{en}|A_V|^2 + S_{enVS}\left(\frac{R_{DUT}}{R_{DUT}+R_B}\right)^2 |A_V|^2, \tag{8}$$

where S_{enDUT}, S_{en} and S_{enVS} are the PSD of e_{nDUT}, e_n and e_{nVS}, respectively. The reason why we did not remove the contribution from e_{nVS} as we have done for e_{nRB} is that, depending on how V_S is implemented, especially at low frequencies, the PSD of e_{nVS} can be large and remain significant even after the attenuation due to the condition $R_{DUT} \ll R_B$. If, on the other hand, a low noise voltage source or batteries are used for V_S, the equivalent input voltage background noise (S_{IVBN}), that can be obtained from Eq. (8) dividing by the modulus of the voltage gain squared in the absence of the contribution by the DUT, becomes:

$$S_{IVBN} = S_{en}. \tag{9}$$

That is, it can essentially be reduced to the contribution of the equivalent input voltage noise source of the operational amplifier.

Note that if the DUT is set in the same bias point in Figs. 4 and 5, the following is true:

$$S_{enDUT} = S_{iDUT}R_{DUT}^2. \tag{10}$$

Let us also assume that the operational amplifiers in Figs. 4 and 5 are the same and that we operate in the conditions for which Eq. (6) holds (low DUT impedance). In these conditions, we have, for the signal to noise ratio in the two circuits:

$$\frac{S_{enDUT}}{S_{IVBN}} = \frac{S_{enDUT}}{S_{en}} = \frac{S_{iDUT}R_{DUT}^2}{S_{en}} = \frac{S_{iDUT}}{\frac{S_{en}}{R_{DUT}^2}} = \frac{S_{iDUT}}{S_{iIBN}}. \tag{11}$$

That is, as we have anticipated above, the two measurement approaches (TIA vs VA) have the same performances in terms of sensitivity. In order to further increase the sensitivity of the measurement system for the same OA we can however resort to cross correlation approaches, and these are more easily implemented using voltage amplifiers.

3.3. Cross correlation approach

The estimation of the PSD S_V of a random stationary signal $V_n(t)$ in frequency ranges up to several tens or hundreds of kHz can be obtained starting from the Discrete Fourier Transform (DFT) of discrete sequences $V_n(i)$ obtained by sampling the signal $V_n(t)$ at regular time instants $t_i = i\Delta T$ with $\Delta T = 1/f_S$ where f_S is the sampling frequency [37]. If $V_n(k)$ is the DFT of the sequence of N samples $V_n(i)$, we obtain an estimate of S_V at certain discrete frequencies f_k as follows:

$$S_v(f_k) = C\cdot\{V_n(k)\cdot V_n^*(k)\},\ f_k = \frac{k}{N}f_S,\ 0 \le k < \frac{N}{2}, \tag{12}$$

where C is a constant that depends on N and of the window function used prior to DFT transformation [37]. More precisely, $S_V(f_k)$ as obtained from Eq. (12) is an estimate of the average of the actual PSD of the signal over bandwidth in the order of $\Delta f = f_S/N$ across the frequency f_k. The quantity Δf is normally referred to as the Resolution Band-Width (RBW), and it is also the lowest frequency (other than 0) for which an estimate can be obtained. The estimation obtained from Eq. (12) is a quite crude one and indeed the estimations obtained from several sequences from the input signal need to be averaged in order to reduce the estimation error. The estimation error for $S_V(f_k)$ from a single sequence is in the same order as the value of the PSD to be estimated and decreases with the square root of the number M of sequences over which $S_V(f_k)$ is averaged. This means that in order to reach an estimation error in the order of 10%, the values of $S_V(f_k)$ relative to 100 sampled sequences must be averaged. Note that the duration of a sequence of length N is $1/\Delta f$, and this means that the overall duration time of measurement (for reaching a given accuracy) is inversely proportional to the resolution bandwidth.

In the estimation of the PSD of the voltage signal at the output of an amplifier (for instance, V_o in Fig. 5), there is no way to separate the contribution due to the DUT from the contribution due to BN of the system. We must therefore insure by design that the BN is much lower than the noise generated by the DUT. Methods exist that allow to subtract the BN noise from the measurements, provided that the BN in the absence of the DUT can be accurately measured and provided that the BN does not change between the two measurements. These approaches are typically time consuming and are effective when the BN is a small portion of the measured noise. Methods based on the same principle that is capable of extracting the correct level of the noise even in the presence of a BN in the same range or even larger than the noise produced by the DUT have been proposed, but they are rather complex, time consuming, and cannot be easily generalized [38].

If two nominally identical VA are available, however, one can take advantage of the properties of cross correlation to reduce the background noise of the system below the BN of a single amplifier.

With reference to Fig. 3, let us assume for the sake of simplicity that the only relevant sources of noise are the noise produced by the DUT at the input of the system (e_{nDUT}) and the equivalent input voltage noise sources e_{n1} and e_{n2} at the inputs of the voltage amplifiers A_1 and A_2. Assuming a very large input impedance for the amplifiers and assuming the gains be equal and constant ($A_1 = A_2 = A$, with A a real and positive value), the output voltages $v_1(t)$ and $v_2(t)$ would be given by:

$$\begin{aligned} v_1(t) &= Ae_{nDUT}(t) + Ae_{n1}(t) \\ v_2(t) &= Ae_{nDUT}(t) + Ae_{n2}(t). \end{aligned} \tag{13}$$

Since the processes $e_{n1}(t)$ and $e_{n2}(t)$ are independent (due to physically separated systems) and, hence, uncorrelated, the cross spectrum S_{12} would be:

$$S_{12} = A^2 S_{nDUT}. \tag{14}$$

That is, the contribution from the equivalent noise sources of the amplifiers is completely rejected.

In actual measurements, however, the rejection of the uncorrelated contribution requires averaging the estimates of the cross spectrum over a sufficiently long time. Cross spectra estimation using DFT proceeds similarly to PSD estimation, save that two sequences of length N are involved, obtained by sampling the outputs $v_1(t)$ and $v_2(t)$. Once the DFTs $V_1(k)$ and $V_2(k)$ are obtained, the estimation of the cross spectrum $S_{12}(k)$ at each frequency f_k is obtained as follows:

$$S_{12}(f_k) = C\cdot\{V_1(k)\cdot V_2^*(k)\},\ f_k = \frac{k}{N}f_S,\ 0 \le k < \frac{N}{2}. \tag{15}$$

In the estimation in Eq. (15), obtained using a single sequence for each channel, there is essentially no rejection of the contribution of the uncorrelated signals. The contributions from the uncorrelated signals, however, decrease with the square root of the number sequences over which the quantity S_{12} is averaged. In principle, an infinite number of records need to be averaged in order to completely reject the uncorrelated noise contribution. In actual measurements, what we need to reach is a situation in which the contribution of the uncorrelated noise becomes much smaller than the noise to be measured. Suppose we observe the evolution of the cross spectrum vs. time (i.e., vs. the number of averages) in a frequency interval in which we expect white noise and in a situation in which the uncorrelated noise is larger than the correlated one. We would initially observe a spectrum whose average value would decrease with time, with a relative standard deviation essentially unchanged, until we reach a level of noise corresponding to the correlated component, at which point further averaging causes a reduction in the standard deviation of the recorded spectrum, without changing the average value [39]. This means that in cross correlation measurement, we initially have to average cross spectra in order to reduce the apparent noise level, and only after we reach the level corresponding to the correlated noise, further averaging results in the reduction of the standard deviation of the estimated spectra. This means that depending on the level of the uncorrelated noise with respect to the correlated one, cross correlation measurement can result extremely time consuming. Say, for instance, that the contribution of the uncorrelated noise is 10 dB above the noise of the DUT to be measured. After 100 averages, the uncorrelated noise contribution to the cross spectrum being estimate is in the same order of the noise of the DUT. After 10^4 averages, the uncorrelated contribution becomes much smaller (-10 dB) than the noise to be measured. In principle, the uncorrelated noise can be much higher than the noise to be measured, and, provided a sufficient number of averages is performed, we can always reject the uncorrelated noise and obtain a correct estimate do the noise from the DUT. It is clear, however, that if the DUT noise is too small with respect to the equivalent input noise of each amplifier, the number of required averages (and the measurement time) becomes unmanageable, especially at low frequencies where a small resolution bandwidth is required and, hence, the duration of each record ($1/\Delta f$) increases. This is why, even if cross correlation is being used, one must start from voltage amplifiers with the lowest possible level of equivalent input noise voltage. It must be noted, however, that if the contribution of the equivalent input noise voltage source of the voltage amplifiers are rejected, this means that the other sources of noise that we have neglected in Section 3.2 and that introduce correlated contributions (among these i_{n1} in Fig. 5 and the noise comping from the bias system), set the actual limit to the BN level that can be reached.

Table 2
"Low noise" opamps.

Type	Input architecture	e_n [nV/√Hz]	i_n [fA/√Hz] at 1 kHz	$R_n = e_n/i_n$[Ω] at 1 kHz	GBW* [MHz]	NF 1 kHz with 1 kΩ *DUT***	C_{CM} [pF]***
AD743	JFET (BiFET)	5.5 at 10 Hz, 3.2 at 1 kHz	6.9	463.8 k	4.5	2.13	18
AD745	JFET (BiFET)	5.5 at 10 Hz, 3.2 at 1 kHz	6.9	463.8 k	20	2.13	18
ADA4625	JFET	5.5 at 10 Hz, 3.3 at 1 kHz	4.5	733.3 k	18	2.23	16.3
TLC070	MOSFET	28 at 10 Hz, 7 at 1 kHz	0.6	11.7 M	10	6.01	22.9
LT1028A	BJT	1.0 at 10 Hz, 0.85 at 1 kHz	1000	850	75	0.47	5
AD797	BJT	1.7 at 10 Hz, 0.9 at 1 kHz	2000	450	110	1.15	5

* gain-bandwidth product.
** calculated noise factor (NF) assuming noninverting configuration with 80 dB gain (set by 10 Ω and 9.99 kΩ resistors) in temperature of 25 °C at 1 kHz.
*** common-mode capacitance.

3.4. Analyses of two-channels electronics design

A two-channel low noise amplifier for cross correlation voltage noise measurements can be built using operational amplifiers only. While cross correlation allows, in principle, to eliminate the contribution of the equivalent input source e_n, the averaging time required to reach a given sensitivity depends on the magnitude of such noise source. It would therefore be advantageous to select OAs with the lowest possible level of e_n for the first gain stage. On the other hand, the contribution to the BN due to the equivalent input current noise i_n cannot be rejected by cross correlation and therefore, depending on the source impedance, the level of i_n may end up being the most important parameter to be aware of in the design of amplifiers for cross correlation voltage noise measurements. Some popular OAs employed in low noise applications are listed in Table 2, with the indication of the input stage technology (BJT, JFET, MOSFET), the values of e_n and i_n, the calculated characteristic noise resistance R_n, the noise figure NF at 1 kHz for a 1 kΩ DUT resistance and the equivalent input capacitance. The characteristic noise resistance can be regarded as the source resistance for which the output noise contributions by e_n and i_n are the same for a conventional single stage voltage amplifier: as far as the source impedance is below R_n, the BN of the amplifier is mostly due to e_n, while above R_n it is mainly i_n that sets the BN of the amplifier. From Table 2, it is apparent that the lowest level of e_n is obtained with BJT input stages, while the highest level of e_n is typically observed in MOSFET input stages. However, as far as the level of i_n, is concerned, the converse is true: the lowest level of i_n is observed in MOSFET input stages, while BJT input stages are characterized by high levels of current noise. As we have mentioned above, in cross correlation applications, we would like to work with low values of e_n in order to reduce the averaging time, but we must select a very low level of i_n if we want the cross correlation approach to be effective at all. With these constraints, it would appear that, among the OA listed in Table 2, the obvious choice for reaching the ultimate level of BN noise would be the TLC070 (lowest level of i_n), notwithstanding its relatively high level of e_n. At the same time, if we are building a system for voltage noise measurement on DUTs whose impedance of which is much smaller than R_n, the JFET input ADA4625 represents a good compromise since it allows for a lower e_n with respect to the TLC070 with an i_n that, assuming a DUT impedance in the order of a few tens of ohms at most, would result in a contribution well below 1 pV/√Hz.

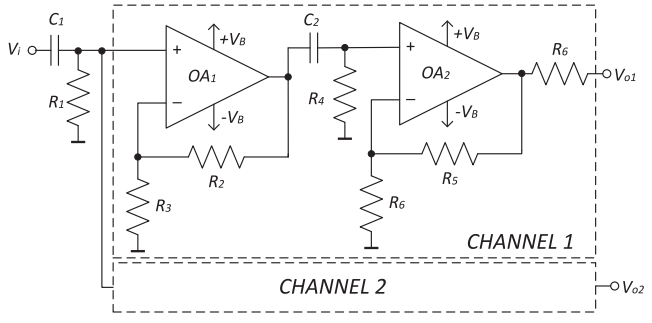

Fig. 6. Schematic diagram of a two-channel low noise voltage amplifier (TCLNVA) for cross correlation measurements based on the ADA4625 operational amplifier. The low-frequency corner is 10 mHz set by the second stage, with an overall gain of 61 dB in the passband.

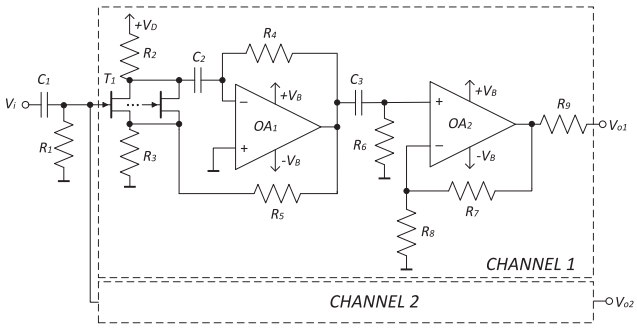

Fig. 7. Schematic diagram of the new two-channel ultra-low-noise voltage amplifier (TCULNVA) for cross correlation noise measurements.

On the basis of this observation, a two-channel low noise voltage amplifier (TCLNVA) based on OA only was built using the ADA4625 OA as shown in Fig. 6. As it will be shown in the next sections, however, the e_n is still too large to obtain sufficiently low BN for our applications. Indeed, the e_n of the ADA4625 at 1 kHz is still 3.3 nV/√Hz, corresponding to the thermal voltage noise of a 700 Ω resistor and, in order to reach an equivalent BN close or below the thermal noise of 1 Ω resistance, the number of averages required in cross-spectra estimation would be in excess of 10^6, which is impractical, to say the least. Therefore, in order to reach the BN required in the case of the measurement of low impedance devices, we must start from amplifiers with a much lower level of e_n, and this can be obtained by resorting to a first stage employing discrete, very low noise JFET devices. As far as the high-frequency limit of TCLNVA is concerned, we have measured a high-frequency corner of about 200 kHz.

The schematic of a two-channel ultra-low-noise voltage amplifier (TCULNVA) developed for the cross correlation set-up in this work is reported in Fig. 7. The structure of the amplifier is similar to an earlier design [40]. The amplifier is consisted of the R_1C_1 filter and two identical amplification channels. The first stage can be regarded as a high gain hybrid amplifier (a discrete JFET transconductance stage followed by an OA based *trans*-resistance stage) in a shunt-series configuration with the feedback network R_5-R_3 setting the voltage gain to A_V=(1 + R_5/R_3).

The input R_1C_1 (10 MΩ and 10 μF) filter has a cut-in frequency of 2 mHz. Such a low-frequency corner is required in order to ensure that the thermal noise of R_1, that is not rejected by cross correlation, is filtered by the capacitor C_1 [16]. The input device T_1 is obtained as the parallel combination of eight 2SK3557-6 JFETs (selected for pinch-off voltage and drain saturation matching), thus obtaining a reduction by a factor of √8 of the equivalent input voltage noise of the amplifier with respect to the case in which a single JFET is used (the equivalent input voltage

noise of 2SK3557-6 is about 1 nV/$\sqrt{\text{Hz}}$ at 1 kHz [40]). With the parallel combination of 8 transistors, the noise introduced by T_1 at 1 kHz becomes comparable to that of the other relevant noise source in the circuit (the resistance $R_3 = 10\ \Omega$). The number 8 was chosen as a compromise among the reduction of the background noise that could be achieved, the space occupied on the printed circuit board and the overall power consumption of the amplifier (that is battery supplied). The resistances R_2 (300 Ω) and R_3 (10 Ω) are wire wound resistors in order to minimize flicker noise (the bias current of the 8 paralleled 2SK3557-6 flows thorough R_2 and R_3). The operational amplifier OA_1 is a low noise LT1028 characterized by a voltage noise of 1 nV/$\sqrt{\text{Hz}}$ at 10 Hz and 0.85 nV/$\sqrt{\text{Hz}}$ at 1 kHz. The cutoff frequency of the C_2R_2 network is 0.1 Hz. With the gain of the first stage set to 52, the noise requirement for the second stage is greatly relaxed. The AC coupling network R_6C_3 (2.2 MΩ and 6.8 μF) with the cut-in frequency of 11 mHz removes the DC offset that can be large because of the presence of T_1 (cut-in frequency 2 mHz). The second stage is a voltage amplifier built around the low noise JFET input OA ADA4625 that is characterized by a voltage noise of 5.5 nV/Hz at 10 Hz and 3.3 nV/Hz at 1 kHz. The overall amplification of the system in the passband is 68.6 dB. The −3dB bandwidth is about 340 kHz.

Taking into consideration the paralleled transistors at the input, the expected voltage noise should be reduced by a factor of $\sqrt{8}$ with respect to that of a single JFET. However, as we have noted above, due to the thermal noise introduced by R_3 (0.4 nV/$\sqrt{\text{Hz}}$), the total input equivalent voltage noise is higher. The estimated equivalent voltage noise level is about 0.55 nV/$\sqrt{\text{Hz}}$ (3×10^{-19} V^2/Hz) at 1 kHz.

3.5. Assessment of the performances of the amplifiers.

The assessment of the performances of the dual-channel amplifier set-ups that we have discussed in the previous paragraph was carried out by performing preliminary measurements for the determination of their bandwidth and their Equivalent Input Voltage Noise (EIVN). The PSD of EIVN for each channel (1st and 2nd ones) in the TCLNVA and TCULNVA is shown in Fig. 8a and 8b, respectively. The spectra were obtained by shorting the input of the amplifiers to the ground. Actual spectral estimation was performed at the outputs of the amplifiers using an SR770 FFT single-channel spectrum analyzer. In order to explore the entire frequency range below 1 Hz up to 100 kHz, measurements were repeated on the same amplifier using different frequency ranges in order to obtain the proper resolution bandwidth in each one of them (the SR770 is capable of a max of 400 frequency points regardless of the frequency span being selected). As it was expected, in the case of TCLNVA, the EIVN essentially coincides with the equivalent input voltage noise of the operational amplifier used in the first stage. In the case of TCULNVA, we obtain a much lower EIVN due to the presence of the paralleled JFETs in the input stage.

In order to perform cross spectrum measurement, we require a two-channel spectrum analyzer. This was obtained by resorting to a PCI-4462 Dynamic Signal Analyzer acquisition board by National Instruments for anti-aliasing filtering and simultaneous sampling and acquisition of the voltages at the output of the amplifiers. A MATLAB script was used for spectral analysis starting from the acquired data. In a first experiment aimed at comparing the performances between TCLNVA and TCLUNVA, we set a resolution bandwidth of $\Delta f = 1.5$ Hz with a sampling frequency of 50 kHz and a record length of 2^{15} samples. The noise floor of the PCI-4462 board is below 10 nV/$\sqrt{\text{Hz}}$ ($f > 10$ Hz) that, accounting for the voltage amplifier gain, translates in a negligible contribution of less than a 4 pV/$\sqrt{\text{Hz}}$ to the equivalent input background noise.

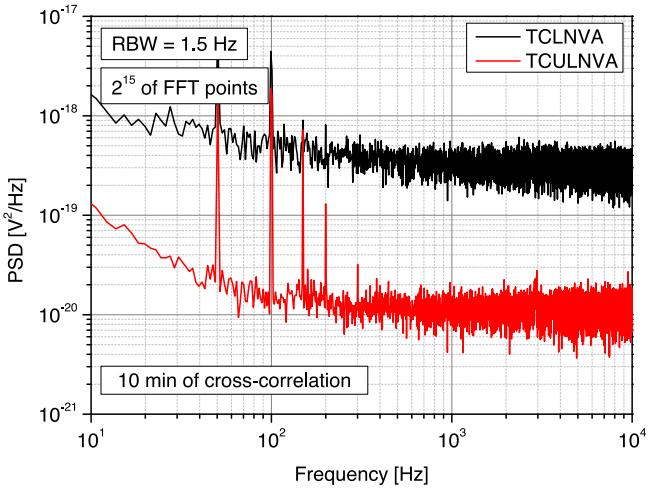

Fig. 9. Equivalent input noise (inputs grounded) obtained by means of cross correlation measurement for the TCLNVA and TCULNVA amplifiers in the same measurement conditions (resolution bandwidth and measurement time).

The result of cross spectra estimation (with the inputs shorted to ground) and a total average time of 10 min is reported in Fig. 9. While it is apparent that through cross spectra estimation, the equivalent EIVN of the amplifier based on OAs only - TCLNVA we can reach, after 10 min, an EIVN that is better than the EIVN of a one single channel of TCULNVA amplifier (Fig. 8a), it is also apparent that by starting from an intrinsically lower EIVN in cross correlation measurements, an extremely low level of equivalent EIVN can be reached in a reasonable time. With reference to Fig. 9, a voltage noise of 10^{-20} V^2/Hz is equivalent to the thermal voltage noise of a 0.6 Ω resistance. By increasing the measurement time, or by increasing the RBW for the same measurement time, even lower equivalent values of EIVN can be reached, the limit being the available time for performing the measurement and, of course, the presence of correlated noise components between the amplifiers in the TCULNVA configuration.

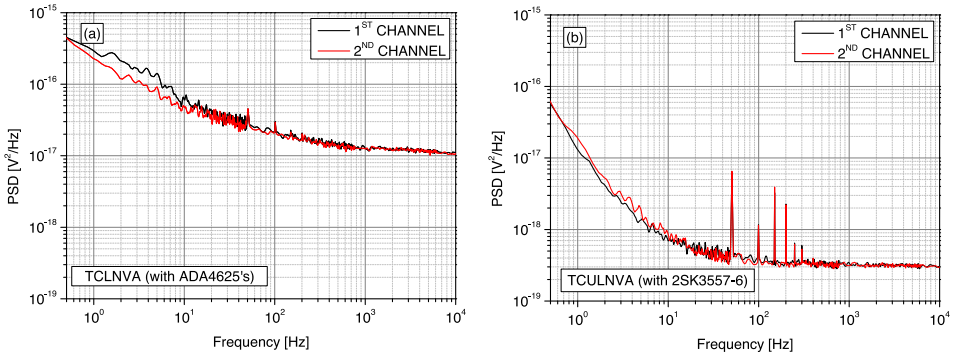

Fig. 8. Input referred voltage noise PSD for each channel in TCLNVA (a) and in TCULNVA (b).

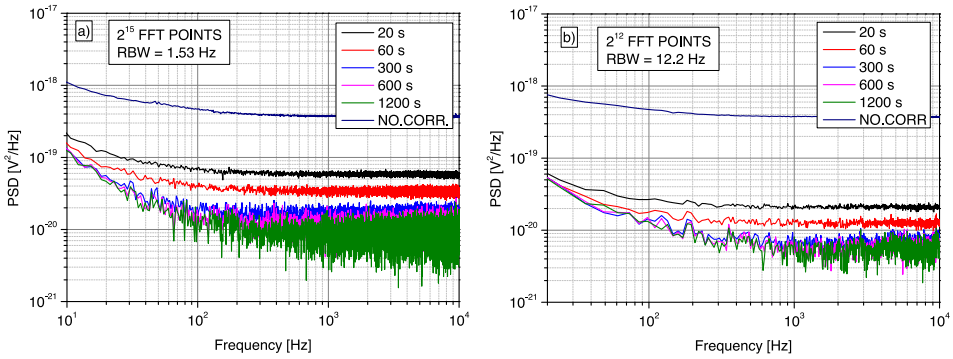

Fig. 10. Equivalent input voltage noise of the designed TCULNVA with 2SK3557-6 JFETs vs. correlation time (T_m) with RBW = 1.53 Hz (a) and 12.2 Hz (b).

Increasing the RBW means that more averages can be performed in the same measurement time because the duration of each time record (1/RBW) is shorter. On the other hand, increasing the RBW means that we lose resolution and accuracy in the low-frequency region of the spectrum [41]. Typically, depending on the application at hand, one must reach a compromise in terms of RBW and the required measurement time for obtaining a given BN. The situation is clearly shown in Fig. 10, where we have plotted the resulting equivalent EIVN from cross spectra noise measurements on TCULNVA vs. measurement time for two different values of RBW. Starting with Fig. 10, we have made the choice of removing the peaks due to the mains interference (50 Hz and harmonics) from the measured spectra in order to simplify the interpretation of the results. It is quite apparent that, for the same measurement time, a much larger reduction in the EIVN is obtained for the larger RBW. At the same time, however, in order to have a correct estimate of the flicker in the low-frequency region, we should operate with RBW much lower than the minimum frequency of interest, which means that the PSD values below 100 Hz in Fig. 10b should be regarded as possibly inaccurate [41]. We also notice that we tend to reach a limiting lower level for the EIVN (this is most clearly noticeable in Fig. 10b), and this means that we have reached the limit at which the correlated noise component dominates the EIVN and it is no longer useful to extend the duration of the measurements. It is worth noticing that with the amplifiers we have designed, we can reach an ultimate noise level in the order of 5.5×10^{-21} V^2/Hz (74 $pV/\sqrt{Hz}$) at frequencies above 1 kHz, and this can be regarded as an excellent result.

4. Results

4.1. Preparation of the measurement setup

Prior to performing noise measurements on actual IR photodetectors, the performances of the noise measurement systems based on the described two-channel amplifier were assessed using known resistors as DUTs. The overall equivalent input noise PSDs were evaluated in the frequency range from 1 Hz up to 100 kHz with a sampling frequency of 204.8 kS/s and a record length of 2^{19} points, resulting in RBW of 0.4 Hz.

The results in Fig. 11a are obtained with the TCULNVA design and a measuring time of 30 min. For each test resistor, we plot the theoretical noise (corresponding to the thermal noise of the resistance at room temperature), the noise estimated from one single amplifier channel (no cross spectrum, S11 in Fig. 11), and the noise obtained from the cross spectrum (S12 in Fig. 11). It is apparent that for relatively high impedances ($\geq$1 k Ω) there is no advantage in performing cross correlation, as the DUT noise is large compared to the EIVN of a single amplifier. As the DUT resistance decreases, the advantage in performing cross correlation becomes apparent, and for resistances down to 10 Ω we can obtain an essentially correct estimation of the DUT noise in the frequency region where the residual $1/f$ noise is not dominant. Note that even with a DUT resistance of 1.5 Ω we obtain an estimation for the DUT noise that is quite close to the correct one (for $f > 100$ Hz), especially when we take into account the fact that, besides the ultimate value of the BN that cannot be reduced by cross correlation, as observed in the

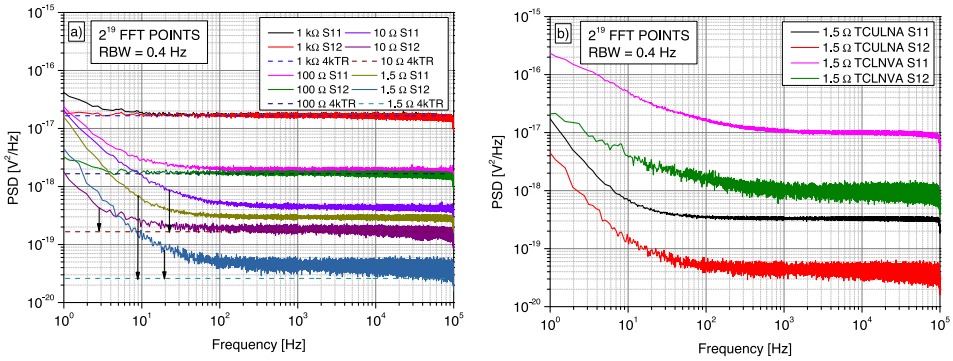

Fig. 11. Test of cross correlation for different resistors used as DUTs. Measurement time was 30 min in all cases. Fig. 11 (a) is obtained using the TCULNVA. Fig. 11 (b) is a comparison between the results with the new TCULNVA and the results that can be obtained with TCLNVA (OA based amplifiers) in the case of a 1.5 Ω resistor used as a DUT.

previous paragraph, the wiring that connects the DUT to the input amplifier can be easily responsible for a parasitic resistance in the order of a significant fraction of 1 Ω whose thermal noise adds to that of the actual DUT connected at the input of the amplifier.

Note that the ability to design a very low noise voltage amplifier to begin with (TCULNVA), even when planning to employ cross correlation, is a key enabling factor if the noise in low impedance DUTs needs to be measured in a reasonable time. To make this fact apparent, we have reported in Fig. 11b the same results for a 1.5 Ω resistor, together with the result that would be obtained, in the same measurement conditions, if the amplifier based on OAs would be used (TCLNVA). As it can be noted, even after 30 min of averaging, the estimated noise in the case of the OAs only (curve TCLNVA S12 in Fig. 11b) is more than one order of magnitude higher than the true value at all frequencies.

4.2. Measurement of InAsSb IR photodetectors noise

The measurements setup discussed above was applied to test InAsSb detectors. These devices are unipolar barrier detectors (nBp) with n-type doped $InAs_{0.85}Sb_{0.15}$ absorber layer, AlAsSb wide-bandgap barrier for electrons, and heavily doped InAsSb N+ (bottom) and P+ (top) contact layers [42]. Such structure increases the efficiency of photogenerated carrier collection and reduces both the dark current and noise of the detector. Moreover, the surface leakage currents because of the presence of a self-passivation layer are also minimized, especially at higher operating temperatures (HOT) (200–300 K). The dynamic resistance area product (R_0A) of commercially available $InAs_xSb_{1-x}$ diodes optimized for middle wavelength infrared (MWIR) detection at 300 K varies from 0.2 to 0.01 Ωcm^2 (with $0 \leq x \leq 0.18$). The low resistances of the detectors are due to the large area of the chip (1 mm^2). Detectors made of III-V materials system with active area ~ 1 mm^2 require additional thermoelectric cooling (TEC) cooling for better operation (to increase their resistance). That is why the production of TEC cooled detectors requires testing of the chip before final hermitization to reduce the costs. Performing such measurements is challenging due to the low detector resistance at 300 K. Proper methods and instrumentation for facilitating noise measurement at room temperature 300 K can therefore be extremely valuable for the implementation of diagnostic tools to check out quality of the devices before final hermitization.

Two samples (DET#1 and DET#2) of low resistance IR photodetectors were tested using the measurement setup in Fig. 12.

These detectors have the same construction with an active area of 1x1 mm (Fig. 13a). The detector chip with the TEC cooler, temperature sensor, and pins for external connection are enclosed in a hermitized metal TO-8 case (Fig. 13b).

At zero bias voltage, the R_0A products at 300 K equal 0.027 Ωcm^2 and 0.035 Ωcm^2 for DET#1 and DET#2, respectively (average values for detectors from the same wafer). For detector biasing, the low noise and stable voltage source described in [43] was used. The detector was

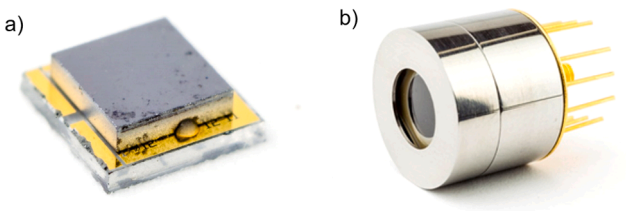

Fig. 13. Detector structure (a) and the detector with integrated TEC in its hermetic TO-8 package (b).

placed on a heat sink whose temperature was stabilized at of 298 K with an accuracy of 1 K. The biasing resistance R_B (30 Ω in case of DET#1 and 60 Ω for DET#2) was a wire-wound resistor in order to avoid additional *1/f* noise. The noise contribution and the attenuation due to the bias resistance was carefully taken into account in the estimation of the PSD generated by the DUT because the simplifying condition of the bias resistance being much larger than the DUT resistance is not verified in this particular case. The voltage across the DUT goes to the input of the TCULNVA amplifier in Fig. 7. The entire measurement chain was placed inside a metal shielding box. Two isolated BNC connectors provide for the connection of amplified output signals to the data acquisition board (PCI-4462).

The results of noise measurements on the two low-impedance InAsSb IR detectors using the TCULNVA are shown in Fig. 14. The DET#1 structure is optimized for a 4.5 μm wavelength with an active area of 1 × 1 mm and is characterized by a shunt resistance of about 4 Ω at 300 K (no bias). The DET#2 has the same parameters, but for its shunt resistance that is about 6 Ω at 300 K.

Noise measurements were performed at equilibrium (no bias voltage) and for increasing bias levels without exceeding the maximum rated values for the devices. Measurement time was 30 min in all cases. The entire time record was first acquired and stored and then analyzed offline using MATLAB. The record length for spectral estimation was 2^{19} that, at the maximum sampling frequency of 204.8 kS/s, results in an explored frequency range up to about 100 kHz with RBW of 0.4 Hz. For each measurement, we plot in Fig. 14 both PSD estimated at the output of one channel (S11) and the result of cross-spectra estimation (S12). This allows to appreciate the advantage of cross correlation and the bias and frequency regions where it is most useful. Bias voltage and current though the DUT are indicated in the legends in Fig. 14a and 14b.

When no bias is applied, we expect thermal (white) noise only coming from the DUT. As it is apparent from Fig. 14, the residual flicker noise in the equivalent EIVN of the amplifier prevents a correct estimation of the equilibrium noise at frequencies below 100 Hz even when cross correlation is used. In the frequency range in which the flicker noise is negligible, the noise level obtained from cross spectra (7.4×10^{-20} V^2/Hz and 1.07×10^{-19} V^2/Hz for DET#1 and DET#2, respectively) are very close to the expected values of the thermal noise

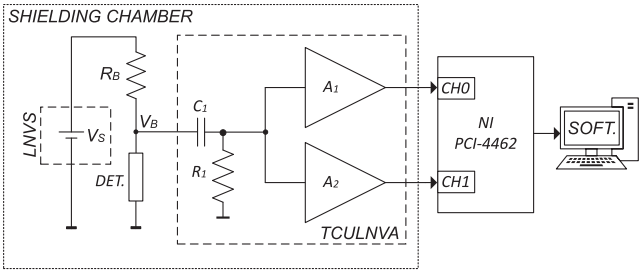

Fig. 12. IR detector noise measurement setup.

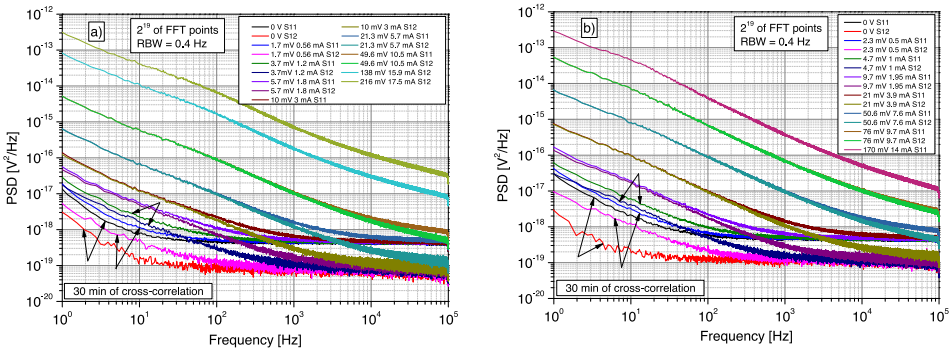

Fig. 14. PSD of voltage fluctuations for InAsSb detectors at 298 K: DET#1 (a) and DET#2 (b) (arrows - results for the same biasing voltages). Each couple of connected arrows points to spectrum and cross spectrum curves from the same measurement.

corresponding to 4 and 6 Ω resistances. From the analysis of Fig. 14, it is clear that, notwithstanding the excellent performances of single amplifier in TCULNVA, without resorting to cross correlation there would be no way to obtain a correct estimate of the noise produced by the DUT in the entire explored frequency range for all intermediate biases. Clearly, as the bias increases, the noise generated by the DUT increases as well and therefore, whenever the noise generated by the DUT is large compared to the noise introduced by each single amplifier, cross-spectra estimation provides essentially the same result as conventional single-channel PSD estimation.

Recording the noise signals in the time domain and performing spectral estimation off-line as we have done to obtain Fig. 14 is useful in that we can process the recorded data using different parameters for spectral estimation, using for instance, different compromises between resolution bandwidth and the number of averages. Moreover, we can employ quite long record lengths that are not normally available in benchtop spectrum analyzers in order to obtain, in a single run, the estimation of the spectra in a wide frequency range (five decades in the case of the spectra in Fig. 14). On the other hand, with this procedure, we lose the ability to monitor the estimation process in real-time, which is especially useful, in the case of cross correlation, to detect when sufficient averaging has been performed, and the measurement can be stopped. Ideally, we would like to retain the ability to store the measurement data in the time domain while retaining the ability of monitoring the status of spectral estimation in real-time and over a wide frequency range. To reach this goal, we have resorted to the public domain QLSA library [44]. QLSA, that stands for Quasi Logarithmic Spectrum Analyzer, provides a simple Application Programming Interface (API) for the design of measurement applications dealing with multi-channel spectra and cross spectra estimation. The QLSA library essentially behaves as a number of virtual, multichannel, conventional benchtop analyzers all working in parallel on the input signals. Each Virtual Spectrum Analyzer (VSA) works with the same record length (typically $N = 4096$ samples). If f_S is the actual sampling frequency, the first analyzer VSA1 works directly on the input signal with a frequency resolution $\Delta f_1 = f_S/N$; the second analyzer, VSA2 works with the same N on a decimated by 4 input signal, with a frequency resolution $\Delta f_3 = f_S/(4\,N)$; the third analyzer, VSA3 works with the same N on a decimated by 16 input signal, with a frequency resolution $\Delta f_3 = f_S/(16\,N)$ and so on, with a factor of 4 in the decimation of the input signal at each step. This results in a number of spectra in which the resolution bandwidth is proportional to the maximum frequency for each VSA, hence the name QLSA. The entire process is transparent to the user, whose task is only to send, in real-time, the acquired stream of data to the QLSA engine and to periodically get the results of spectra estimation according to parameters set by the user. The results of noise measurements on DET#1, in the same condition as for the measurements in Fig. 14a, when QLSA is used for spectral estimation is reported in Fig. 15. As it can be noticed, each curve is the result of the combination of the estimates obtained by the different VSAs operating within QLSA. For the sake of clarity in the representation, only the outputs of odd order VSAs were used (VSA1, VSA3, VSA5, etc.). All the portions of the spectrum corresponding to single bias voltage were obtained in real-time and at the same time. Using QLSA, we can therefore follow the evolution of the spectra in real-time, over about six frequency decades with the most proper resolution bandwidth in each frequency range. It is apparent that at higher frequencies, the spectra are smoother as the result of the larger resolution bandwidth (larger number of averages for the same measurement time) and become less smooth as we need to decrease the resolution bandwidth in the lower frequency region. It is important to notice that for obtaining the estimation of the spectrum from 0.1 Hz to about 100 kHz as in Fig. 15 using the conventional approach, the record length should have been set to at least 2^{22} and since the resolution bandwidth would have been the same at all frequencies, we would have obtained the same statistical fluctuations in the spectrum, that can be noticed in the lowest frequency range in Fig. 15, at all frequencies. The fact that by using QLSA, we can monitor the evolution of the spectra estimation process in real-time and over a large bandwidth is extremely useful in all those conditions in which the ability to maintain stable condition for the DUT during measurements can be challenging. For instance, in the case in which measurement at cryogenic temperatures must be performed, the ability to maintain constant temperature conditions by resorting to liquid nitrogen is limited in time and to avoid drifts and hence artifacts in the spectra, we must be able to monitor the progress of the

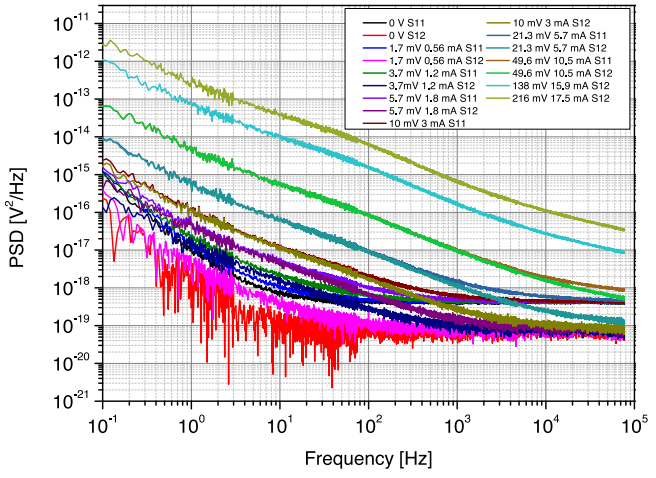

Fig. 15. Results for DET #1 InAsSb detector at 298 K (Resistance ≈ 4 Ω) when a spectrum analyzer based on QLSA software is used. Notice that, with respect to Fig. 14, the frequency axis extends down to 0.1 Hz.

measurements and stop the test as soon as we notice that sufficiently smooth spectra are obtained in all frequency regions we may be interested in.

Overall, using a QLSA based spectrum analyzer greatly simplifies performing noise measurements over a wide frequency range and significantly contributes to take full advantage of the ultra-low noise measurement approach we have developed in this work.

5. Summary and outlook

We have developed an ultra-low noise measurement system for the investigation of the noise produced by devices characterized by low shunt resistance. After discussing why the most appropriate approach in this case is to resort to cross correlation voltage noise measurements, we have developed a hybrid ultra-low noise amplifier that, by introducing an extremely low level of voltage noise, when used in a cross correlation configuration, allows to considerably reduce the measurement time required to reject the uncorrelated components.

Indeed, with the TCULNVA amplifier, we have developed, with measurements lasting 600 s, at frequencies above 1 kHz, we can reach an equivalent voltage noise as low as 74 and 100 $pV/\sqrt{Hz}$ when setting the frequency resolution for cross spectra estimation to 12.2 Hz and 1.5 Hz, respectively.

The system has been validated by performing noise measurement onto advanced IR photodetectors, and the ability to perform meaning low frequency noise measurement on a wide frequency range and for a wide range of bias conditions had been demonstrated. Using advanced software tools for spectral estimation, the ability to perform real-time noise measurements over six frequency decades (0.1 Hz–100 kHz) in a single measurement session has also been demonstrated.

CRediT authorship contribution statement

Krzysztof Achtenberg: Conceptualization, Investigation, Methodology, Resources, Software, Writing - original draft. **Janusz Mikołajczyk:** Formal analysis, Validation, Writing - review & editing. **Carmine Ciofi:** Supervision, Writing - review & editing, Software, Validation. **Graziella Scandurra:** Validation, Writing - review & editing. **Krystian Michalczewski:** Resources. **Zbigniew Bielecki:** Writing - review & editing, Supervision, Validation.

Declaration of Competing Interest

The authors declare that they have no known competing financial interests or personal relationships that could have appeared to influence the work reported in this paper.

Acknowledgments

This work was supported by the Military University of Technology grant number ZBW/08-896/2020/WAT.

References

[1] L.K.J. Vandamme, Noise as a diagnostic tool for quality and reliability of electronic devices, IEEE Trans. Electron Devices 41 (1994) 2176–2187.
[2] L. Ciura, A. Kolek, J. Jurenczyk, K. Czuba, A. Jasik, I. Sankowska, E. Papis-Polakowska, J. Kaniewski, Noise-current correlations in InAs/GaSb Type-II superlattice midwavelength infrared detectors, IEEE Trans. Electron Devices 63 (2016) 4907–4912, https://doi.org/10.1109/TED.2016.2620181.
[3] G.R. Savich, J.R. Pedrazzani, D.E. Sidor, S. Maimon, G.W. Wicks, Dark current filtering in unipolar barrier infrared detectors, Appl. Phys. Lett. 99 (2011).
[4] C. Cervera, I. Ribet-Mohamed, R. Taalat, J.P. Perez, P. Christol, J.B. Rodriguez, Dark current and noise measurements of an InAs/GaSb superlattice photodiode operating in the midwave infrared domain, J. Electron. Mater. 41 (2012) 2714–2718, https://doi.org/10.1007/s11664-012-2035-4.
[5] Ł. Ciura, M. Kopytko, P. Martyniuk, Low-frequency noise limitations of InAsSb-, and HgCdTe-based infrared detectors, Sensors Actuators, A Phys. 305 (2020) 1–6, https://doi.org/10.1016/j.sna.2020.111908.
[6] Ł. Ciura, A. Kolek, J. Jureńczyk, K. Czuba, A. Jasik, I. Sankowska, J. Kaniewski, 1/f Noise modeling of InAs/GaSb superlattice mid-wavelength infrared detectors, Opt. Quantum Electron. 50 (2018) 1–11, https://doi.org/10.1007/s11082-017-1308-9.
[7] D. Ramos, M. Delmas, R. Ivanov, L. Höglund, E. Costard, P.E. Hellström, G. Malm, 1/f Noise and Dark Current Correlation in Midwave InAs/GaSb Type-II Superlattice IR Detectors, Phys. Status Solidi Appl. Mater. Sci. 2000557 (2020), https://doi.org/10.1002/pssa.202000557.
[8] L. Ciura, A. Kolek, K. Michalczewski, K. Hackiewicz, P. Martyniuk, *1/f* Noise in InAs/InAsSb Superlattice Photoconductors, IEEE Trans. Electron Devices. 67 (2020) 3205–3210, https://doi.org/10.1109/TED.2020.2998449.
[9] X. Zhong, S. Keshavarz, J. Jones, C. Mewes, P.R. Leclair, Cross-spectrum Analyzer for Low Frequency Noise Analysis, (n.d.) 1–10.
[10] Y. Dai, A precision noise measurement and analysis method used to estimate reliability of semiconductor devices, Microelectron. Reliab. 37 (1997) 893–899, https://doi.org/10.1016/s0026-2714(96)00117-5.
[11] Y. Chen, C.M. Van Vliet, P.M. Koenraad, G.L. Larkins, Lorentzian noise in the two-dimensional electron gas of AlxGa1-xAs/GaAs quantum wells, J. Appl. Phys. 86 (1999) 6206–6212, https://doi.org/10.1063/1.371732.
[12] C. Ciofi, G. Giusi, G. Scandurra, B. Neri, Dedicated instrumentation for high sensitivity, low frequency noise measurement systems, Fluct. Noise Lett. 4 (2004), https://doi.org/10.1142/S0219477504001963.
[13] L. Baracchino, G. Basso, C. Ciofi, B. Neri, Ultralow-noise programmable voltage source, IEEE Trans. Instrum. Meas. 46 (1997) 1256–1261, https://doi.org/10.1109/19.668267.
[14] G. Scandurra, G. Giusi, C. Ciofi, A very low noise, high accuracy, programmable voltage source for low frequency noise measurements, Rev. Sci. Instrum. 85 (2014), https://doi.org/10.1063/1.4870248.
[15] G. Scandurra, G. Giusi, C. Ciofi, A programmable bias current compensation approach in current noise measurement applications, Conf. Rec. - IEEE Instrum. Meas. Technol. Conf. (2019–May (2019)) 1–5, https://doi.org/10.1109/I2MTC.2019.8826981.
[16] G. Scandurra, G. Cannatà, G. Giusi, C. Ciofi, A new approach to DC removal in high gain, low noise voltage amplifiers, 2017 Int. Conf. Noise Fluctuations, ICNF 2017 (2017), pp. 1–4. https://doi.org/10.1109/ICNF.2017.7985946.
[17] G. Scandurra, G. Giusi, C. Ciofi, Single JFET Front-End Amplifier for Low Frequency Noise Measurements with Cross Correlation-Based Gain Calibration, Electronics 8 (10) (2019) 1197, https://doi.org/10.3390/electronics8101197.
[18] F.A. Levinzon, Ultra-low-noise high-input impedance amplifier for low-frequency measurement applications, IEEE Trans. Circuits Syst. I Regul. Pap. 55 (2008) 1815–1822, https://doi.org/10.1109/TCSI.2008.918213.
[19] B. Neri, B. Pellegrini, R. Saletti, Ultra Low-Noise Preamplifier for Low-Frequency Noise Measurements in Electron Devices, IEEE Trans. Instrum. Meas. 40 (1991) 2–6, https://doi.org/10.1109/19.69939.
[20] Ł. Ciura, A. Kolek, W. Gawron, A. Kowalewski, D. Stanaszek, Measurements of low frequency noise of infrared photodetectors with transimpedance detection system, Metrol. Meas. Syst. 21 (2014) 461–472, https://doi.org/10.2478/mms-2014-0039.
[21] 5182 Current Preamplifier - Instruction Manual, www.ameteksi.com.
[22] K. Hackiewicz, Ł. Ciura, P. Ptak, P. Martyniuk, J. Rutkowski, A. Kolek, Low frequency noise of mid-wavelength interband cascade photodetectors up to 300 K, SPIE Defense + Commercial Sensing, Proceedings Volume 11002, Infrared Technol. Appl. XLV (2019) 87, https://doi.org/10.1117/12.2520038.
[23] K. Jaworowicz, C. Cervera, J.B. Rodriguez, P. Christol, Noise Characterization of Midwave Infrared InAs / GaSb Superlattice pin Photodiode, IEEE Photon. Technol. Lett. 23 (4) (2011) 242–244, https://doi.org/10.1109/LPT.2010.2093877.
[24] R. Taalat, P. Christol, J. Rodriguez, Dark Current and Noise Measurements of an InAs/GaSb Superlattice Photodiode Operating in the Midwave Infrared Domain, J. Electron. Mater. 41 (2012), https://doi.org/10.1007/s11664-012-2035-4.
[25] 5113 Low Noise Voltage Preamplifier - Instruction Manual, www.ameteksi.com.
[26] N. Dyakonova, S.A. Karandashev, M.E. Levinshtein, B.A. Matveev, M.A. Remennyi, Low frequency noise in p-InAsSbP / n-InAs infrared photodiodes, Semicond. Sci. Technol. 33 (6) (2018).
[27] N. Dyakonova, S.A. Karandashev, M.E. Levinshtein, B.A. Matveev, M.A. Remennyi, Low frequency noise in reverse biased P- InAsSbP / n- InAs infrared photodiodes, Semicond. Sci. Technol. 34 (1) (2019).
[28] M. Sampietro, G. Accomando, L.G. Fasoli, G. Ferrari, E.C. Gatti, L. Fellow, High Sensitivity Noise Measurement with a Correlation Spectrum Analyzer, IEEE Trans. Instrum. Meas. 49 (2000) 820–822.
[29] M. Sampietro, L. Fasoli, G. Ferrari, Spectrum analyzer with noise reduction by cross-correlation technique on two channels, Rev. Sci. Instrum. 70 (1999) 2520–2525, https://doi.org/10.1063/1.1149785.
[30] A. Wörl, F. Rutz, R. Rehm, J.-M. Masur, P. Kleinow, J. Schmitz, J. Niemasz, W. Luppold, T. Stadelmann, M. Walther, T. Simon, R. Scheibner, J. Ziegler, 2.4 - Electro-Optical Properties of InAs/GaSb Superlattice Infrared Photodiodes for Bispectral Detection, Proc. IRS2 2013 (2020) 37–42, https://doi.org/10.5162/irs2013/i2.4.
[31] L. Zhu, J. Huang, Z. Xie, Z. Deng, L. Chen, C. Lin, B. Chen, Low-frequency noise spectroscopy characterization of HgCdTe infrared detectors, IEEE Trans. Electron Devices 67 (2020) 547–551, https://doi.org/10.1109/TED.2019.2960281.
[32] C. Meng, J. Li, L. Yu, X. Wang, P. Han, F. Yan, Z. Xu, J. Chen, X. Ji, Investigation of a noise source and its impact on the photocurrent performance of long-wave-infrared InAs/GaSb type-II superlattice detectors, Opt. Express 28 (2020) 14753, https://doi.org/10.1364/oe.386920.
[33] L. Zhu, Z. Deng, J. Huang, H. Guo, L. Chen, C. Lin, B. Chen, Low frequency noise-dark current correlations in HgCdTe infrared photodetectors, Opt. Express 28 (2020) 23660, https://doi.org/10.1364/oe.399565.

[34] M. Razeghi, A. Haddadi, G. Chen, A.M. Hoang, R. Chevallier, F. Callewaert, Low-frequency noise in mid-wavelength infrared InAs/GaSb type-II superlattice based focal plane arrays, Infrared Technol. Appl. XL. 9070 (2014) 90701H, https://doi.org/10.1117/12.2057505.
[35] A. Wörl, R. Rehm, M. Walther, Excess noise in InAs/GaSb type-II superlattice pin-photodiodes, Infrared Phys. Technol. 61 (2013) 5–8, https://doi.org/10.1016/j.infrared.2013.06.010.
[36] TLC070, TLC071, TLC072, TLC073, TLC074, TLC075, TLC07xA Family of wide-bandwidth high-output-drive single supply operational amplifiers - Datasheet, www.ti.com.
[37] P. Welch, The Use of Fast Fourier Transform for the Estimation of Power Spectra: A Method Based on Time Averaging Over Short, Modified Periodograms, Audio Electroacoust., IEEE Trans. 15 (1967) 70–73, https://doi.org/10.1109/TAU.1967.1161901.
[38] M. Macucci, B. Pellegrini, Very Sensitive Measurement Method of Electron Device Current Noise, IEEE Trans. Instrum. Meas. 40 (1991) 7–12, https://doi.org/10.1109/19.69940.
[39] J. Briaire, L.K.J. Vandamme, Uncertainty in Gaussian noise generalized for cross-correlation spectra, J. Appl. Phys. 84 (1998) 4370–4374, https://doi.org/10.1063/1.368657.
[40] K. Achtenberg, J. Mikołajczyk, Z. Bielecki, FET input voltage amplifier for low frequency noise measurements, Metrol. Meas. Syst. 27 (2020) 531–540, https://doi.org/10.24425/mms.2020.132785.
[41] G. Giusi, G. Scandurra, C. Ciofi, Estimation errors in 1/fγ noise spectra when employing DFT spectrum analyzers, Fluct. Noise Lett. 12 (2013) 1–22, https://doi.org/10.1142/S0219477513500077.
[42] A. Rogalski, P. Martyniuk, M. Kopytko, P. Madejczyk, S. Krishna, InAsSb-based infrared photodetectors: Thirty years later on, Sensors (Switzerland). 20 (2020) 1–74, https://doi.org/10.3390/s20247047.
[43] K. Achtenberg, J. Mikołajczyk, C. Ciofi, G. Scandurra, Z. Bielecki, Low-noise programmable voltage source, Electron 9 (8) (2020) 1–13, https://doi.org/10.3390/electronics9081245.
[44] C. Ciofi, G. Scandurra, G. Giusi, QLSA: A Software Library for Spectral Estimation in Low-Frequency Noise Measurement Applications, Fluct. Noise Lett. 18 (2019) 1940004, https://doi.org/10.1142/S0219477519400042.